JACS
JOURNAL OF THE AMERICAN CHEMICAL SOCIETY

Communication

pubs.acs.org/JACS

Label-Free Aptasensor Based on Ultrathin-Linker-Mediated Hot-Spot Assembly To Induce Strong Directional Fluorescence

Shuo-Hui Cao,[†] Wei-Peng Cai,[†] Qian Liu,[†] Kai-Xin Xie,[†] Yu-Hua Weng,[†] Si-Xin Huo,[†] Zhong-Qun Tian,[‡] and Yao-Qun Li*[,†]

[†]Department of Chemistry and the MOE Key Laboratory of Spectrochemical Analysis & Instrumentation, College of Chemistry and Chemical Engineering, Xiamen University, Xiamen 361005, China

[‡]State Key Laboratory of Physical Chemistry of Solid Surfaces, College of Chemistry and Chemical Engineering, Xiamen University, Xiamen, 361005, China

Supporting Information

ABSTRACT: We have demonstrated the proof-of-concept of a label-free biosensor based on emission induced by an extreme hot-spot plasmonic assembly. In this work, an ultrathin linking layer composed of cationic polymers and aptamers was fabricated to mediate the assembly of a silver nanoparticles (AgNPs)−dyes−gold film with a strongly coupled architecture through sensing a target protein. Generation of directional surface plasmon coupled emission (SPCE) was thus stimulated as a means of reporting biorecognition. Both the biomolecules and the nanoparticles were totally free of labeling, thereby ensuring the activity of biomolecules and allowing the use of freshly prepared metallic nanoparticles with large dimensions. This sensor smartly prevents the plasmonic assembly in the absence of targets, thus maintaining no signal through quenching fluorophores loaded onto a gold film. In the presence of targets, the ultrathin layer is activated to link NPs−film junctions. The small gap of the junction (no greater than 2 nm) and the large diameter of the nanoparticles (∼100 nm) ensure that ultrastrong coupling is achieved to generate intense SPCE. A >500-fold enhancement of the signal was observed in the biosensing. This strategy provides a simple, reliable, and effective way to apply plasmonic nanostructures in the development of biosensing.

The hot-spot structure involving plasmonic interactions has attracted much attention. A remarkable plasmonic coupling effect has been reported to occur in the nanometer interstices between metallic nanostructures, accompanied by special plasmon-mediated optical phenomena.[1] For instance, in surface-enhanced Raman spectroscopy (SERS), the plasmonic coupling effect at a nanometer gap junction between metallic structures is now known to generate enormous electromagnetic enhancement, thereby allowing the SERS signal to be detected with single-molecule sensitivity.[2] Enhanced plasmon-mediated fluorescence has been observed when a fluorescent molecule is placed at the center of metallic structures in close proximity.[3] Our recent work has revealed that fluorescence in the form of surface plasmon coupled emission (SPCE) can be triggered by a hot-spot structure, which broadens the influence of plasmonic interactions on emitters.[4]

The number of literature reports of biomolecule detection methods that employ hot-spot geometries has been rapidly increasing, reflecting the potential of utilizing these dramatic optical properties for clinical diagnostics and biomolecular interaction studies.[5] However, great challenges impede the further development of sensitive and reliable chemical/biological sensing techniques based on hot-spot structures. First, plasmonic coupling is dependent on distance, and it decreases dramatically with an increase in the plasmonic gap of a few nanometers.[1d,6] As a result, enormous plasmonic coupling, in principle, requires that the gap distance be reduced as much as possible. Actually, a gap with a separation distance less than 2 nm approaches the ultimate limits of plasmonic enhancement;[1d,7] however, to take advantage of bio-interactions (specific binding events), researchers commonly utilize biomolecules such as proteins to link plasmonic junctions.[4,5b,8] In these designs, the lengths of metallic gaps are determined by the size of the biomolecules bound inside, typically greater than several nanometers or even tens of nanometers in diameter (e.g., those used in sandwich immunoassays). This size limitation restricts the electromagnetic enhancement coupling, which requires plasmonic interaction at the closest range. Second, the majority of current biosensor designs require biofunctionalized metallic nanostructures.[4,5b,8] Therefore, the activity and affinity of biological molecules for recognition may be more prone to be diminished. Third, the stability of nanostructures may be affected after functionalization. In particular, the difficulty is increased when biofunctionalizing nanoparticles with a large diameter while maintaining good colloidal stability in the saline conditions required for bioaffinity interactions.[9] Thus, this difficulty limits the applications of large nanoparticles, which usually exhibit strong electromagnetic field enhancement in plasmonic interactions.[10] In summary, these bottlenecks have impeded access to controlled, effective experimental studies within the high-coupling hot-spot regime (separation distance <2 nm)[7] for biosensing applications.

To meet these challenges, we herein propose a label-free platform of ultrastrong plasmonic coupling for biosensing. An aptasensor based on ultrathin layer linked nanoparticles (NPs)-on-film hot-spot plasmonic assembly to induce directional

Received: January 28, 2014
Published: May 2, 2014

dx.doi.org/10.1021/ja500976a | J. Am. Chem. Soc. 2014, 136, 6802−6805

SPCE is established as the proof-of-concept. Nucleic acid aptamers are certain sequences of DNA formed via in vitro selection techniques to bind targets with high affinity and specificity and have great advantages in the development of selective biosensors.[11] SPCE is the plasmon-mediated fluorescence in which excited fluorophores couple with a metallic thin film through near-field interactions to form the emitting species, termed plasmophores, and then radiate to the far field in a specific direction.[12] NPs−film junctions are considered to be a controllable hot-spot structure in practice.[1d,5b,7] Here, aptamers, together with cationic polymers, are designed to form an ultrathin layer. This layer serves as both the sensing layer to targets and the linking layer between the NPs and the film, and it mediates the assembly of AgNPs on the dye-coated gold surface while triggering strong SPCE. Both the biomolecules and the NPs are completely label-free during the sensing processes. This design provides a simple and reliable approach to the construction of a biorecognition-induced extreme hot-spot structure.

The fundamental concept of this approach is illustrated in Figure 1. The ultrathin linker is conveniently fabricated through depositing one layer of cationic polymers and one layer of aptamers successively on the dye-coated smooth gold surface. Initially, it is negatively charged because of the abundant negative charges on the outermost layer of aptamers. As a result, in the absence of targets, the freshly synthesized, negatively charged AgNPs could not be assembled on the surface because of the huge electrostatic repulsion. In this case, no signal is detected because the fluorescence is quenched. In contrast, in the presence of targets to which aptamers have higher affinity than to cationic polymers, the positive charges from embedded cationic polymers are exposed, leading to the assembly of AgNPs on the surface. Therefore, the occurrence of biorecognition correlates to the assembly of plasmonic nanostructures without the need for biomolecules as direct linkers. Furthermore, the close-connected sandwich architecture of NPs−dyes−film is a highly effective hot-spot structure that induces enormous plasmonic coupling to generate directional SPCE.

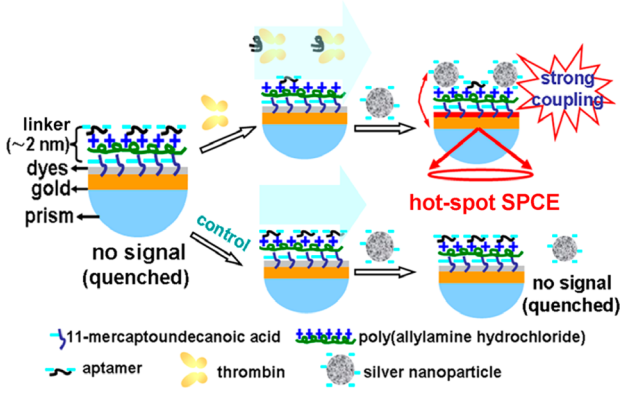

Figure 1. Schematic illustration of the aptasensor based on ultrathin layer linked hot-spot SPCE to detect the target protein. When the target is added to interact with the aptamer, the positively charged polymers are exposed and can catch the negatively charged AgNPs. The close-connected hot-spot plasmonic architecture will induce directional SPCE. When the target is absent, the negatively charged surface will smartly hinder the assembly of the hot-spot architecture; thus, there is no signal to be detected. Images are not drawn to scale.

The experimental steps are described below. The smooth gold nanofilm was fabricated by depositing a 2 nm adhesive layer of chromium and a 50 nm layer of gold onto a quartz substrate, which was attached with an index-matching fluid to a prism positioned on a precise rotary stage in a homemade multifunctional spectrofluorimeter for SPCE detection.[4,11a,12d] The gold surface was immersed for 12 h in 100 μM cysteamine and 1 mM 11-mercaptoundecanoic acid mixed together in ethanol. The surface was therefore modified with amino groups and carboxyl groups. The amino groups were present for the connection of dyes, and the carboxyl groups were present for the adsorption of cationic polymers. After the surface was rinsed, 100 μM rhodamine B isothiocyanate in a carbonate buffer (pH 9.0) was added, and the surface was immersed for 6 h, resulting in the dyes directly coating the gold surface. The fluorophores were immobilized on the chip substrate, which greatly simplified the operation compared to that used for traditional biosensors, where fluorophores are labeled to biomolecules. The black curve in Figure 2a indicates that the dyes were completely quenched in proximity to the gold surface because of nonradiative energy transfer.[13] Then, 1 μg/mL of poly(allylamine hydrochloride) (PAH) was added onto the surface for 2 h, and the surface was subsequently rinsed. PAH is positively charged; it can therefore be adsorbed onto the carboxyl-modified surface to form a monolayer rich in positive charges.[6a] Next, a 1.4 μM thrombin-binding aptamer (sequences: GGTTGGTGTGGTTGG) in a TE buffer (0.5 M NaCl, 10 mM Tris, 0.5 mM EDTA, pH 7.6) was used to incubate the surface overnight. The negatively charged phosphate backbone of the DNA aptamer induced adsorption of the aptamer to the oppositely charged polymers on the surface.[14] After the appropriate quantity of aptamers was added, the surface was dominated by negative charges. The sample solution was then added to immerse the surface under gentle shaking for 30 min. If thrombin is present in the solution, the aptamers will specifically interact with it because of their high affinity, and the distribution of surface charges will thus be changed.[15] On the contrary, the interface is still negatively charged in the control experiment. After being rinsed, the freshly prepared AgNPs were added onto the surface and incubated for 30 min. The spherical AgNPs with an average particle size of 100 nm were prepared according to the modified Lee−Meisel method through citrate reduction and were negatively charged.[16] The green curve in Figure 2a indicates that the fluorescence was completely quenched in the absence of targets because the negatively charged aptamers greatly repelled the similarly charged AgNPs. This result means that the nonspecific adsorption was effectively suppressed, which should be attributable to the stability of the untreated AgNPs and to the reasonable interfacial design. The red curve indicates that strong fluorescence was observed after thrombin was sensed, thereby indicating the occurrence of strong plasmonic coupling. The typical result presented in Figure 2b reveals that, in the reverse Kretschmann (RK) configuration, where light is incident on the front of the sample interface, emission was strongly directional, at 46° relative to the normal axis through the prism after thrombin was sensed. The emission was observed to be p-polarized (Figure S3). The directional and highly p-polarized emission demonstrates that coupling occurs between the fluorophores and plasmons, because only a defined angle and p-polarized emission can satisfy the requirements of wave-vector matching.[12] Moreover, directional SPCE has the advantage of more efficient hot-spot coupling,

dx.doi.org/10.1021/ja500976a | J. Am. Chem. Soc. 2014, 136, 6802−6805

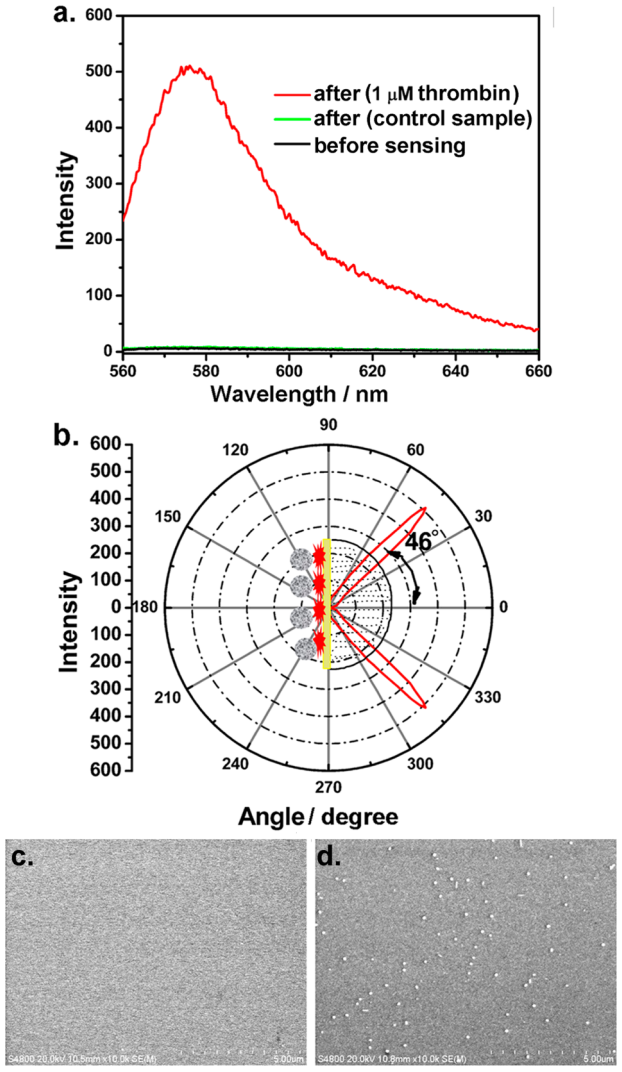

Figure 2. (a) Signals before (black line) and after the control sample (green line) and a 1 μM thrombin sample (red line) were sensed. (b) Angular distribution of the directional SPCE signal after a 1 μM thrombin sample was sensed. (c) SEM image of the chip surface after the control sample was sensed. (d) SEM image of the chip surface after a 1 μM thrombin sample was sensed, showing that the NPs–film assembly had formed.

showing an ~10-fold enhancement compared to isotropic free space emission (FSE) observed from the air side of the gold film (Figure S4). As presented in Figure 2c,d, scanning electron microscopy (SEM) was used to investigate the microstructures of the chip surface after sensing. No NPs were observed in the SEM image when the control sample was used, whereas NPs were easily discerned on the chip surface by SEM in the presence of thrombin. Thus, the appearance of the directional SPCE signal is attributed to a thrombin-stimulated interfacial response, through which the ultrathin linker was activated to mediate the assembly of NPs–dyes–film, creating highly effective hot-spots through NPs–film junctions.

The extreme hot-spot SPCE should be related to the strong plasmonic coupling in the hot-spot structure.[4] Nanoparticles can be used to enhance electromagnetic fields,[17] and the NPs–film structure combines both localized and propagated surface plasmons by greatly concentrating electromagnetic coupling in the gap.[2c,7,18] We used finite-difference time domain (FDTD) to calculate and evaluate the electromagnetic field in the NPs–film structures. We observed that the electromagnetic field obviously decreased as the diameter of the AgNPs was reduced (Figure S6). The freshly prepared 100 nm AgNPs without further modification support strong surface plasmon resonance. The ultrathin linker (no more than 2 nm, as shown in Figure S5) between the NPs and film plays an important role in ensuring strong plasmonic coupling. The electromagnetic field decreased when the gap was enlarged (Figure S7). As observed in the previous model detection,[4] the SPCE signal decreased by almost 90% when the NPs–film gap was increased to ~35 nm, though it is still obvious compared to the weak FSE signal. As a result, the hot-spot SPCE biosensor based on the ultrathin layer achieves the maximum benefit from plasmonic coupling. The ultrathin-linker-mediated hot-spot SPCE can be considered as one kind of NPs–film gap-mediated emission. The emission rate has the potential to surpass the nonradiative decay rate at close emitter–metal spacings, and the strong plasmonic coupling emission from the gap structure should be resistant to quenching.[3d,19] An enhanced electromagnetic field, a net increase in emission efficiency, and an improved collective efficiency from directional radiation[20] contribute to the strong hot-spot SPCE.

The sensing response was evaluated on the basis of the increase in the signal, which was calculated as $R = (F_{after} - F_{background})/(F_{before} - F_{background})$, where F_{before} and F_{after} are the detected fluorescence signals before and after the sensing processes and $F_{background}$ is the detected background intensity from the equipment. We observed that the increase in the signal was dependent on the thrombin concentration, with a linear calibration curve of thrombin that spanned 4 orders of magnitude in concentration. The regression equation was $y = 164.7 + 110.3(\lg x)$ ($R^2 = 0.9898$), with a limit of detection of 33 pM (S/N = 3σ, where σ is the standard deviation of the control sample, $n = 11$) (Figure 3a). The selectivity of the

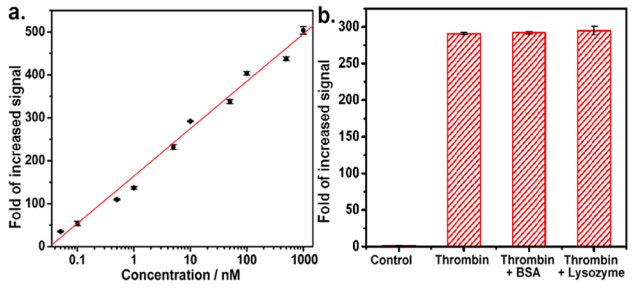

Figure 3. (a) Calibration curve for the increase in signal as a function of the thrombin concentration. (b) Increase in signal with the sensing response to the blank PBS buffer, 10 nM thrombin, 1 μM BSA + 10 nM thrombin, and 1 μM lysozyme + 10 nM thrombin.

sensor was tested. The responses exhibit no obvious influence, even when a 100-fold excess of other proteins were added as interference components to the thrombin samples (Figure 3b). The results also confirm that neither negatively charged proteins (bovine serum albumin) nor positively charged proteins (lysozyme) interfered with the sensing.

In summary, an ultrathin-linker-mediated hot-spot SPCE aptasensor is proposed as a proof-of-concept. The sensor is based on a simple approach that avoids labeling of either the biomolecules or the AgNPs. It utilizes the interfacial interaction in an ingenious way to hinder or trigger the plasmonic assembly of extreme hot-spots. The ultrathin layer, composed of cationic

dx.doi.org/10.1021/ja500976a | J. Am. Chem. Soc. 2014, 136, 6802–6805

polymers and aptamers, acts as both the sensing layer to targets and the linking layer between the NPs and film. It smartly blocks the adsorption of AgNPs in the absence of targets and actively captures AgNPs to form ultrastrong hot-spots in the presence of targets. As a result, it not only exhibits sensing specificity to targets but also manipulates the plasmon-mediated fluorescence in reporting biosensing. Utilizing the ultrathin layer as the linker of hot-spots to reduce the plasmonic gap between the NPs and film, together with the use of freshly prepared large-dimension NPs, the produced ultrastrong plasmonic coupling triggers intense directional SPCE for reporting biosensing, thus guaranteeing a high sensitivity of the biosensor. This work opens new opportunities toward the development of a chip-based platform that utilizes a hot-spot structure in a highly effective manner to create biosensors. It is a general strategy of instructive significance for other plasmon-mediated spectroscopy methods to achieve an ultrastrong hot-spot effect with sufficient sensitivity and controllability.

■ ASSOCIATED CONTENT

Supporting Information

Additional experimental data and simulations. This material is available free of charge via the Internet at http://pubs.acs.org.

■ AUTHOR INFORMATION

Corresponding Author

yaoqunli@xmu.edu.cn

Notes

The authors declare no competing financial interest.

■ ACKNOWLEDGMENTS

Financial support from the National Science Foundation of China (grant nos. 21375111, 21127005), the 973 Program of China (2013CB933703), the funds of the Ministry of Education of China (grant no. 20110121110011, PCSIRT IRT13036), and the excellent doctoral student scholarship award granted by the Ministry of Education of China is gratefully acknowledged. We thank Prof. Bin Ren and Dr. Xiang Wang for providing FDTD calculation support. We thank Prof. Peter Nordlander, Prof. Zhi-Lin Yang, Dr. Song-Yuan Ding, and Mr. Ling-Yan Meng for helpful discussions during the revision of this manuscript.

■ REFERENCES

(1) (a) Yoon, I.; Kang, T.; Choi, W.; Kim, J.; Yoo, Y.; Joo, S.-W.; Park, Q.-H.; Ihee, H.; Kim, B. *J. Am. Chem. Soc.* **2009**, *131*, 758−762. (b) Halas, N. J.; Lal, S.; Chang, W.-S.; Link, S.; Nordlander, P. *Chem. Rev.* **2011**, *111*, 3913−3961. (c) Lim, D.-K.; Jeon, K.-S.; Hwang, J.-H.; Kim, H.; Kwon, S.; Suh, Y. D.; Nam, J.-M. *Nat. Nanotechnol.* **2011**, *6*, 452−460. (d) Ciracì, C.; Hill, R. T.; Mock, J. J.; Urzhumov, Y.; Fernández-Domínguez, A. I.; Maier, S. A.; Pendry, J. B.; Chilkoti, A.; Smith, D. R. *Science* **2012**, *337*, 1072−1074. (e) McMahon, J. M.; Li, S.; Ausman, L. K.; Schatz, G. C. *J. Phys. Chem. C* **2012**, *116*, 1627−1637.

(2) (a) Camden, J. P.; Dieringer, J. A.; Wang, Y.; Masiello, D. J.; Marks, L. D.; Schatz, G. C.; Van Duyne, R. P. *J. Am. Chem. Soc.* **2008**, *130*, 12616−12617. (b) Qian, X.-M.; Nie, S. M. *Chem. Soc. Rev.* **2008**, *37*, 912−920. (c) Hill, R. T.; Mock, J. J.; Urzhumov, Y.; Sebba, D. S.; Oldenburg, S. J.; Chen, S.-Y.; Lazarides, A. A.; Chilkoti, A.; Smith, D. R. *Nano Lett.* **2010**, *10*, 4150−4154. (d) Li, J. F.; Huang, Y. F.; Ding, Y.; Yang, Z. L.; Li, S. B.; Zhou, X. S.; Fan, F. R.; Zhang, W.; Zhou, Z. Y.; Wu, D. Y.; Ren, B.; Wang, Z. L.; Tian, Z. Q. *Nature* **2010**, *464*, 392−395.

(3) (a) Kinkhabwala, A.; Yu, Z.; Fan, S.; Avlasevich, Y.; Mullen, K.; Moerner, W. E. *Nat. Photon.* **2009**, *3*, 654−657. (b) Schmelzeisen, M.; Zhao, Y.; Klapper, M.; Mullen, K.; Kreiter, M. *ACS Nano* **2010**, *4*, 3309−3317. (c) Fu, Y.; Zhang, J.; Lakowicz, J. R. *Langmuir* **2013**, *29*, 2731−2738. (d) Russell, K. J.; Liu, T. L.; Cui, S.; Hu, E. L. *Nat. Photon.* **2012**, *6*, 459−462.

(4) Cao, S. H.; Cai, W. P.; Liu, Q.; Xie, K. X.; Weng, Y. H.; Li, Y. Q. *Chem. Commun.* **2014**, *50*, 518−520.

(5) (a) Cao, Y. C.; Jin, R.; Nam, J.-M. C.; Thaxton, S.; Mirkin, C. A. *J. Am. Chem. Soc.* **2003**, *125*, 14676−14677. (b) Braun, G.; Joon Lee, S.; Dante, M.; Nguyen, T.-Q.; Moskovits, M.; Reich, N. *J. Am. Chem. Soc.* **2007**, *129*, 6378−6379. (c) Wang, Y.; Wei, H.; Li, B.; Ren, W.; Guo, S.; Dong, S.; Wang, E. *Chem. Commun.* **2007**, *43*, 5220−5222. (d) Kim, N. H.; Lee, S. J.; Moskovits, M. *Adv. Mater.* **2011**, *23*, 4152−4156. (e) Zheng, J.; Jiao, A.; Yang, R.; Li, H.; Li, J.; Shi, M.; Ma, C.; Jiang, Y.; Deng, L.; Tan, W. *J. Am. Chem. Soc.* **2012**, *134*, 19957−19960.

(6) (a) Mock, J. J.; Hill, R. T.; Degiron, A.; Zauscher, S.; Chilkoti, A.; Smith, D. R. *Nano Lett.* **2008**, *8*, 2245−2252. (b) Liu, Y.; Xu, S.; Li, H.; Jian, X.; Xu, W. *Chem. Commun.* **2011**, *47*, 3784−3786. (c) Wustholz, K. L.; Henry, A.-I.; McMahon, J. M.; Freeman, R. G.; Valley, N.; Piotti, M. E.; Natan, M. J.; Schatz, G. C.; Van Duyne, R. P. *J. Am. Chem. Soc.* **2010**, *132*, 10903−10910.

(7) Hill, R. T.; Mock, J. J.; Hucknall, A.; Wolter, S. D.; Jokerst, N. M.; Smith, D. R.; Chilkoti, A. *ACS Nano* **2012**, *6*, 9237−9246.

(8) (a) Bonham, A. J.; Braun, G.; Pavel, I.; Moskovits, M.; Reich, N. O. *J. Am. Chem. Soc.* **2007**, *129*, 14572−14573. (b) Kang, T.; Yoo, S. M.; Yoon, I.; Lee, S. Y.; Kim, B. *Nano Lett.* **2010**, *10*, 1189−1193. (c) Han, X. X.; Kitahama, Y.; Itoh, T.; Wang, C. X.; Zhao, B.; Ozaki, Y. *Anal. Chem.* **2009**, *81*, 3350−3355. (d) Wang, Y.; Lee, K.; Irudayaraj, J. *Chem. Commun.* **2010**, *46*, 613−615.

(9) Kwon, M. J.; Lee, J.; Wark, A. W.; Lee, H. J. *Anal. Chem.* **2012**, *84*, 1702−1707.

(10) (a) Lakowicz, J. R. *Anal. Biochem.* **2005**, *337*, 171−194. (b) Ko, H.; Singamaneni, S.; Tsukruk, V. V. *Small* **2008**, *4*, 1576−1599. (c) Chen, A.; DePrince, A. E., III; Demortière, A.; Joshi-Imre, A. *Small* **2011**, *7*, 2365−2371.

(11) (a) Xie, T. T.; Liu, Q.; Cai, W. P.; Chen, Z.; Li, Y. Q. *Chem. Commun.* **2009**, *45*, 3190−3192. (b) You, M. X.; Chen, Y.; Peng, L.; Han, D.; Yin, B. C.; Ye, B. C.; Tan, W. H. *Chem. Sci.* **2011**, *2*, 1003−1010. (c) Du, Y.; Li, B. L.; Wang, E. K. *Acc. Chem. Res.* **2013**, *46*, 203−213.

(12) (a) Lakowicz, J. R. *Anal. Biochem.* **2004**, *324*, 153−169. (b) Previte, M. J. R.; Geddes, C. D. *J. Am. Chem. Soc.* **2007**, *129*, 9850−9851. (c) Lakowicz, J. R.; Ray, K.; Chowdhury, M.; Szmacinski, H.; Fu, Y.; Zhang, J.; Nowaczyk, K. *Analyst* **2008**, *133*, 1308−1346. (d) Cao, S. H.; Xie, T. T.; Cai, W. P.; Liu, Q.; Li, Y. Q. *J. Am. Chem. Soc.* **2011**, *133*, 1787−1789. (e) Cao, S. H.; Cai, W. P.; Liu, Q.; Li, Y. Q. *Annu. Rev. Anal. Chem.* **2012**, *5*, 317−336.

(13) Anger, P.; Bharadwaj, P.; Novotny, L. *Phys. Rev. Lett.* **2006**, *96*, 113002.

(14) (a) Ho, H.-A.; Leclerc, M. *J. Am. Chem. Soc.* **2004**, *126*, 1384−1387. (b) Du, Y.; Chen, C. G.; Li, B. L.; Zhou, M.; Wang, E. K.; Dong, S. J. *Biosens. Bioelectron.* **2010**, *25*, 1902−1907.

(15) (a) Yang, X. H.; Wang, S. F.; Wang, K. M.; Luo, X. M.; Tan, W. H.; Cui, L. *Chem. J. Chin. Univ.* **2009**, *30*, 899−902. (b) Wu, Y.; Zhan, S.; Wang, F.; He, L.; Zhi, W.; Zhou, P. *Chem. Commun.* **2012**, *48*, 4459−4461. (c) Ding, J.; Chen, Y.; Wang, X.; Qin, W. *Anal. Chem.* **2012**, *84*, 2055−2061.

(16) Lee, P. C.; Meisel, D. *J. Phys. Chem.* **1982**, *86*, 3391−3395.

(17) (a) Chowdhury, M. H.; Ray, K.; Geddes, C. D.; Lakowicz, J. R. *Chem. Phys. Lett.* **2008**, *452*, 162−167. (b) Aslan, K.; McDonald, K.; Previte, M. J. R.; Zhang, Y. X.; Geddes, C. D. *Chem. Phys. Lett.* **2008**, *464*, 216−219.

(18) Mock, J. J.; Hill, R. T.; Tsai, Y. J.; Chilkoti, A.; Smith, D. R. *Nano Lett.* **2012**, *12*, 1757−1764.

(19) Russell, K. J.; Hu, E. L. *Appl. Phys. Lett.* **2010**, *97*, 163115.

(20) Ming, T.; Chen, H. J.; Jiang, R. B.; Li, Q.; Wang, J. F. *J. Phys. Chem. Lett.* **2012**, *3*, 191−202.